LETTER

Fabrication of a Metal Membrane on a Perforated Polymer Substrate by Palladium Aerosol Activation and Subsequent Electroless Plating

Jeong Hoon Byeon[†] and Jungho Hwang*[,‡]

Digital Printing Division, Samsung Electronics Company, Ltd., Suwon 443-742, Republic of Korea, and School of Mechanical Engineering and Yonsei Center for Clean Technology, Yonsei University, Seoul 120-749, Republic of Korea

ABSTRACT Fabrication of a metal membrane on a perforated flexible poly(tetrafluoroethylene) (PTFE) substrate was developed by employing spark-generated palladium (Pd) aerosol activation and the subsequent electroless plating of Pd. After aerosol activation, Pd agglomerates of spark-generated primary particles (~2.6 nm in diameter) with a face-centered-cubic structure were deposited uniformly on the PTFE substrate. Homogeneous Pd particles with an average size of 188 nm were tightly packed together to form a Pd membrane after Pd plating. The average plating rate of Pd during 30 min of plating at an activation intensity of 25 $\mu g/cm^2$ was 14.2 $\mu g/cm^2 \cdot$ min.

KEYWORDS: metal membrane • perforated PTFE substrate • spark generation • Pd aerosol activation • electroless plating

1. INTRODUCTION

Metal composite materials ranging from submicron to microscale have received a great deal of interest in many fields, such as catalysis, adsorption science, separation science, purification of macromolecules, biomedical, electronics, and photonics (1−5). The incorporation of metal particles into polymer matrixes is an area of particular interest for the study of interactions between metals and polymers (1, 2). In particular, there has been increasing interest in the preparation of polymer-supported palladium (Pd) nanoparticles because of their much improved catalytic selectivity (6). Among the methods for fabricating thin Pd-based membranes on a polymeric substrate, electroless plating (ELP) has strong advantages over sputtering, chemical vapor deposition, and electrodeposition, particularly with respect to its cost performance, use of nonconductive substrates with complex shapes, and simple equipment (7).

The initiation of the ELP process is preceded by surface activation to provide catalytic sites on the material surface. Activation strongly influences ELP and the quality of the metal membranes. Uniform coverage of the surface with as many small (nanosized) seeds as possible is desired. Concerning conventional tin (Sn)-based activation (8), it was suggested that the introduction of Sn leads to the gradual degradation of the membrane performance due to alloying (9). Moreover, this conventional activation requires a long process time, intermittent water rinsing, and drying. In addition, the process involves the loss of expensive metal ions and creates problems with environmental pollution (10−13). Consequently, it is highly desirable to develop a simple and ecologically attractive activation method prior to the ELP process (14−20). In an attempt to improve catalytic surface activation as an aerosol catalysis (21), Byeon et al. (22) recently reported the catalytic surface activation of activated carbon fibers using Pd aerosol nanoparticles for use in a silver (Ag) ELP. Aerosol activation involves fewer steps than conventional surface activation.

This manuscript introduces fabrication of a metal membrane on a perforated poly(tetrafluoroethylene) (PTFE) substrate by Pd aerosol activation and subsequent Pd ELP. PTFE was selected because it is attractive for use in membrane processes because of its superior chemical resistance, good thermal stability, and high mechanical strength (23−25). Although the extremely hydrophobic property of PTFE typically limits its performance in practical applications (26, 27), aerosol activation enabled particular functional groups to be introduced directly onto the PTFE surface without the need for wet chemical steps. Spark generation (28) was used to produce Pd aerosol nanoparticles under ambient conditions, which were captured by the perforated PTFE substrate by physical filtration. After heating at 240 °C, the catalytically activated substrate was immersed horizontally in a Pd plating bath to form a Pd layer on the activated substrate. Other metal membranes, such as Ag, gold (Au), copper (Cu), and nickel (Ni), were also fabricated using different plating

* Corresponding author. Tel.: (+82-2) 2123-2821. Fax: (+82-2) 312-2821. E-mail: hwangjh@yonsei.ac.kr.
Received for review November 9, 2008 and accepted January 14, 2009
[†] Samsung Electronics Company, Ltd. E-mail: postjb@yonsei.ac.kr.
[‡] Yonsei University.
DOI: 10.1021/am8001742

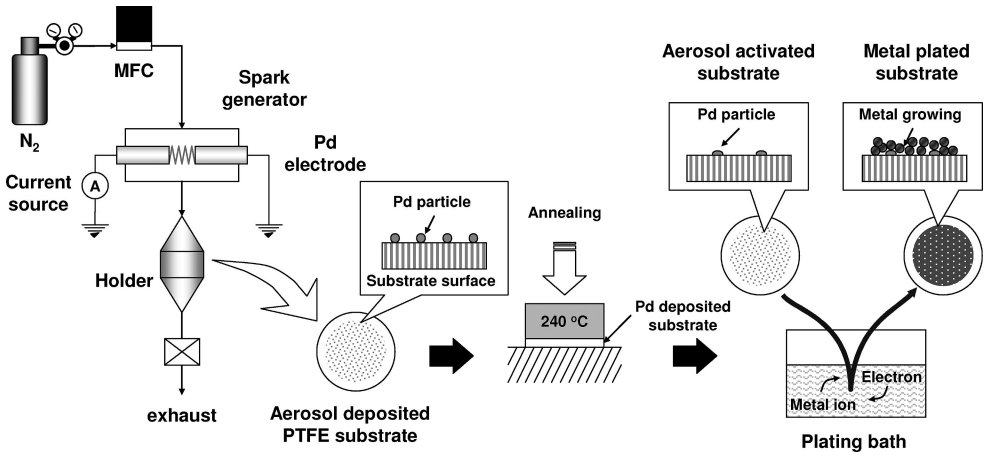

FIGURE 1. Procedure for metal membrane fabrication.

baths because Pd can be used as an alloy with those metals to reduce the incidence of poisoning and embrittlement (29–33).

2. MATERIALS AND METHODS

2.1. Membrane Fabrication. Figure 1 shows a schematic of the method used to fabricate a metal membrane. A spark was generated between two identical Pd rods (diameter = 3 mm, length = 100 mm; Nilaco, Tokyo, Japan) inside a reactor under a pure nitrogen environment at standard temperature and pressure (STP) (22). The electrical circuit specifications were as follows: resistance of 0.5 MΩ, capacitance of 10 nF, loading current of 2.1 mA, applied voltage of 2.8 kV, and frequency of 600 Hz. The gap distance between the electrodes was 1 mm. The spark-generated Pd aerosol nanoparticles were carried by nitrogen gas and deposited onto a perforated flexible PTFE substrate (47 mm in diameter, 0.2 μm in pore size, and 50 μm in thickness, 11807-47-N, Sartorius, Göttingen, Germany). In order to prevent the detachment of nanoparticles from the surface of the substrate, the substrate was annealed in air at 240 °C for 10 min after it was separated from the holder.

Once the substrate had been activated by the aerosol process, the substrate was immersed horizontally in a Pd plating bath (34, 35). Layer growth occurred through the plating of the metals onto the nuclei. Pd plating is an autocatalytic process according to the overall reaction $2Pd(NH_3)_4^{2+} + N_2H_4 + 4OH^- \rightarrow 2Pd^0 + N_2 + 4H_2O + 8NH_3$. The compositions of plating baths and plating conditions were described in Table 1.

2.2. Instrumentation. The size distribution of the Pd aerosol nanoparticles was measured using a scanning mobility particle sizer (SMPS) consisting of an electrostatic classifier (TSI 3085), ultrafine condensation particle counter (TSI 3025), and aerosol charge neutralizer (NRD 2U500). The morphology and microstructure of the spark-generated Pd nanoparticles were analyzed by high-resolution transmission electron microscopy (HRTEM; JEM-3010) operated at 300 kV. X-ray photoelectron spectroscopy (XPS) measurements of the activated substrate were performed using a Kratos Axis HIS spectrometer with a monochromatized Al Kα X-ray source (1486.6 eV photons) at a constant dwell time of 100 ms and a pass energy of 40 eV. Field-emission scanning electron microscopy (JSM-6500F, JEOL, Tokyo, Japan) images and energy-dispersive X-ray spectroscopy (EDX; JED-2300, JEOL, Tokyo, Japan) of the activated and ELP substrates were obtained at an accelerating voltage of 15 kV. The quantity of spark-generated and ELP particles plated on the substrate was determined by inductively coupled plasma atomic emission spectroscopy (ICP-AES; Elan 6000, Perkin-Elmer, Waltham, MA). X-ray diffraction (XRD) of the ELP particles was carried out on a Rigaku RINT-2100 diffractometer equipped with a thin-film attachment using Cu Kα radiation (40 kV, 40 mA). The 2θ angles ranged from 10 to 90° at a scanning speed of 4°/min at an interval of 0.08°. Atomic force microscopy (AFM) was used for the topography of the electroless metal-plated substrate. Topographic images of the substrate were recorded under ambient conditions using a multimode scanning probe microscope connected to a NanoScope IIIa controller.

Table 1. Compositions of Plating Baths and Plating Conditions

ELP	bath composition	bath temperature (°C)
Pd	1.5 g/L of $PdCl_2$, 40.1 g/L of disodium ethylenediaminetetraacetate (Na_2-EDTA · $2H_2O$), 195 mL/L of NH_3 · H_2O (28%), 5 mL/L of N_2H_4 (1 M)	45
Ag	solution A: 2 g/L of $AgNO_3$, 60 g/L of Na_2-EDTA · $2H_2O$, 88 mL/L of isopropyl alcohol, 12 mL/L of acetic acid, 400 mL/L of NH_4OH	20
	solution B: 3 mL/L of hydrazine, 2 mL/L of mercerine, 400 mL/L of ethanol	
	mixture solutions of A and B at 1:1 (v/v)	
Au	5 g/L of $KAu(CN)_2$, 8 g/L of KCN, 20 g/L of NaOH, 10 g/L of glycine, 25 g/L of $NaBH_4$	80
Cu	solution A: 30 g/L of $CuSO_4$, 140 g/L of sodium potassium tartrate (Rochelle salt), 40 g/L of NaOH	20
	solution B: aqueous formaldehyde solution (37.2 wt %)	
	mixture solutions of A and B at 10:1 (v/v)	
Ni	15 g/L of $NiSO_4$ · $6H_2O$, 18 g/L of $H_3C_6H_5O_7$ · $6H_2O$, 30 g/L of NaH_2PO_2 · H_2O, 28 g/L of $NaCH_3COO$ · $3H_2O$, 20 mL/L of latic acid (85%), 2 mg/L of thiourea	70

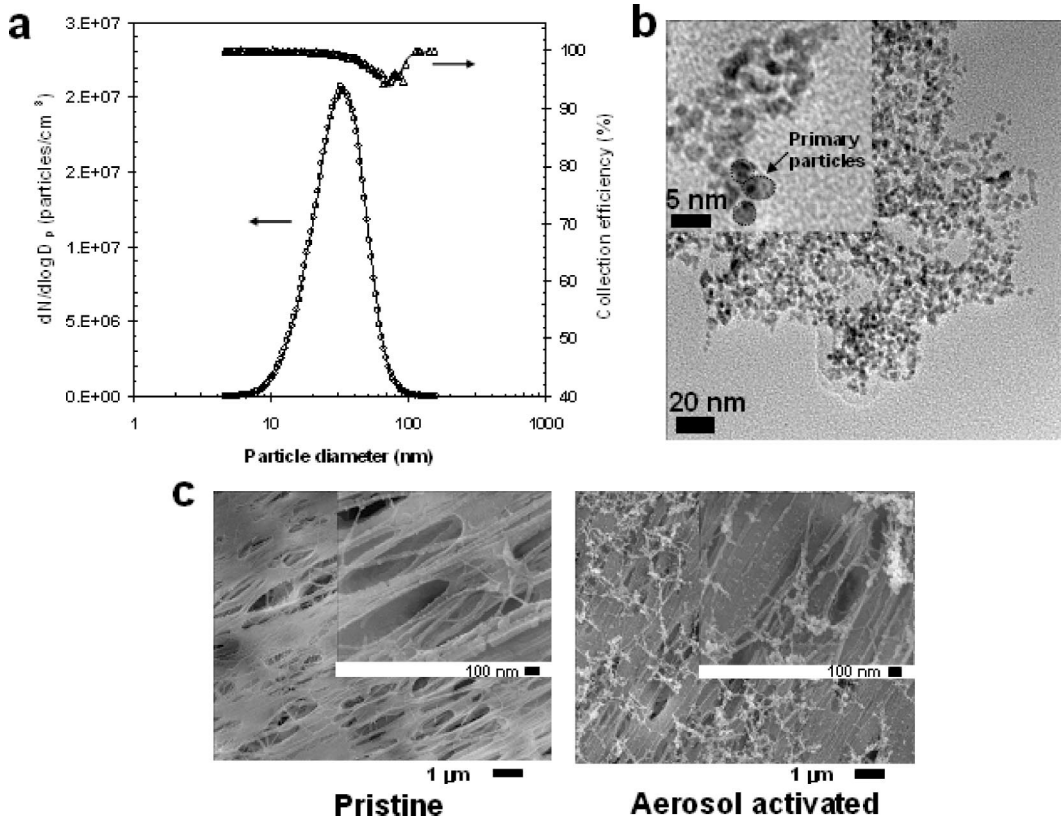

FIGURE 2. Characterizations of aerosol activation: (a) particle size distribution and collection efficiency of aerosol nanoparticles; (b) HRTEM micrographs of aerosol nanoparticles; (c) SEM micrographs of pristine and aerosol-activated substrates.

3. RESULTS AND DISCUSSION

3.1. Activation by Pd Aerosol Nanoparticles. Figure 2a shows the size distribution of the spark-generated Pd aerosol nanoparticles, which was measured with the SMPS system at 20 cm downstream of the spark generator. The geometric mean diameter and geometric standard deviation were 29.3 nm and 1.53, respectively. The total number concentration, total area concentration, and total mass concentration were 9.84×10^6 particles/cm^3, 3.73×10^{10} nm^2/cm^3, and 249 μg/m^3, respectively. Figure 2a also shows the fractional (grade) collection efficiency of the substrate as a function of the particle size, which was calculated using the following equation:

$$\eta(d_p) = 1 - \left[\frac{C_f(d_p)}{C_i(d_p)}\right] \quad (1)$$

where $C_i(d_p)$ is the freestream particle concentration and $C_f(d_p)$ is the concentration after filtration by the substrate. The overall collection efficiency is defined as follows:

$$\eta_{\text{overall}} = \frac{\int_0^\infty \eta(d_p)\, C_i(d_p)\, \mathrm{d}d_p}{\int_0^\infty C_i(d_p)\, \mathrm{d}d_p} \quad (2)$$

The data shown in Figure 2a resulted in $\eta_{\text{overall}} = 98.6\,\%$. The HRTEM micrographs (Figure 2b) show that the spark-generated nanoparticles were agglomerates of primary particles (inset, each ~26 nm in diameter).

SEM (Figure 2c) showed that the pristine substrate had a clean surface, while a number of particles were deposited on the activated substrate. The activation intensity was approximately 25 μg · particle/cm^2 · substrate. In the XPS analyses (not shown), the binding energy doublets of the Pd $3d_{5/2}$ and Pd $3d_{3/2}$ peak components located at approximately 335 and 340 eV, respectively, were assigned to Pd^0 species (36). From the EDX analyses (not shown), it was found that the pristine substrate contained carbon (C, 21.1 % in mass) and fluorine (F, 67.8 % in mass), which may have originated from the substrate, while activated substrate contained a small amount of Pd (11.1 % in mass).

3.2. Fabrication of a Pd Membrane by Pd ELP. The SEM micrographs in Figure 3a show the trend of metal plating on the activated spots of the substrate with a plating time ranging from 10 to 30 min. The electroless particles plated initially on the top of the Pd seeds. The particles had a random orientation resulting in irregular disposition. The number of particles increased progressively with increasing plating time, leading to a more compact coating, which covered most of the substrate surface. The particles shown in Figure 3a were 176−194 nm in size, which depended slightly on the plating time. These results correspond to a recent study reported by Shi et al. (37), where the particle size was almost constant at the same $PdCl_2$ concentration in the plating bath. Figure 3b shows a flattened AFM image of the surface (30 min plating) obtained in the tapping mode. Although there were a few convex sites (so-called island structure), the entire membrane surface was nearly uniform. The thickness and root-mean-squared roughness of the membrane were approximately 1.6 μm and 44.7

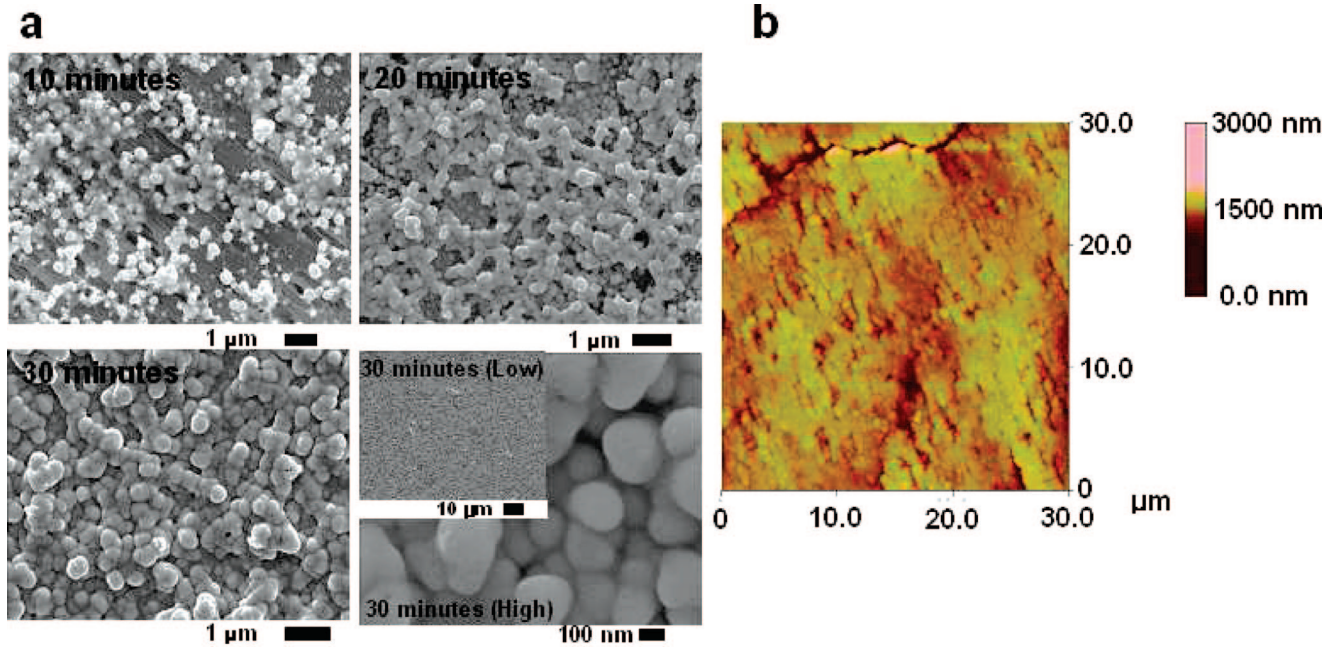

FIGURE 3. Characterizations of Pd ELP: (a) SEM micrographs of electroless particle plated substrates for plating times of 10, 20, and 30 min; (b) AFM topograph of a particle plated substrate for a plating time of 30 min.

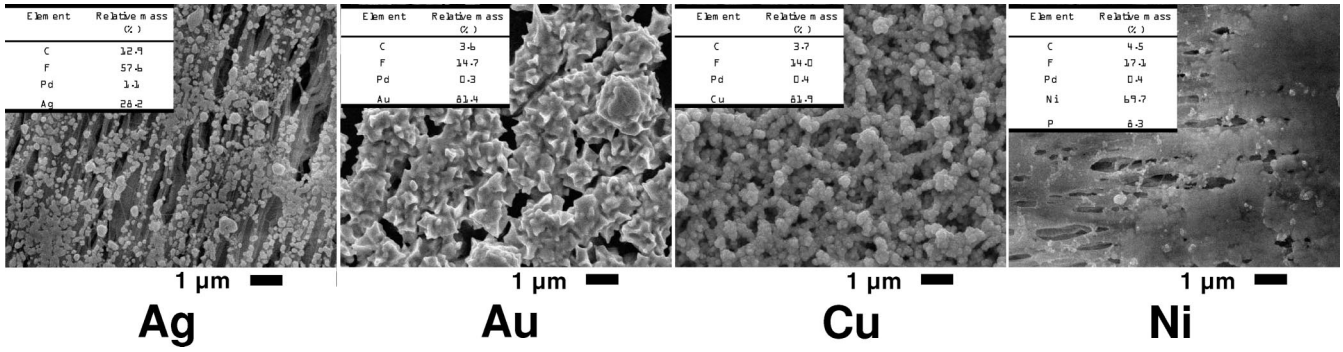

FIGURE 4. Characterizations of other metal membranes after 30 min of plating.

nm, respectively. Therefore, the estimated dimensional growth rate was 53 nm/min for the case of 30 min plating. Assuming that monodisperse particles were packed in a sample geometrical array, the number of particle monolayers was calculated for the case of 30 min plating using the relationship between T, n, and R, as expressed by Shi and Szpunar (37):

$$n = \frac{(T/R) - 1.172}{0.414} \tag{3}$$

where T (nm) is the membrane thickness, n is the number of particle monolayers, and R is the particle radius. The membrane was found to consist of approximately 38 particle monolayers.

From EDX analysis (not shown), it was found that the coated metal was mainly Pd (81.8% in mass). C (4.4% in mass) and F (13.8% in mass), which may have originated from the substrate itself, were also detected. The amounts of Pd membranes were also obtained from ICP-AES analyses. The plating rates for 10, 20, and 30 min of ELP were 14.4, 17.1, and 14.2 $\mu g/cm^2 \cdot$ min, respectively. The results indicated an increase in the plating rate until 20 min plating, which is a characteristic of an autocatalytic reaction (19, 38). The plating rate decreased after prolonged ELP (20−30 min) because of the depletion of reactants in the plating bath. XRD of the Pd particles after 30 min of plating revealed four peaks at $2\theta = 40.6$, 46.4, 68.2, and 82.4°. A comparison of these peaks with the data from the joint committee on powder diffraction standards (JCPDS) file showed these peaks to correspond to the (111), (200), (220), and (311) planes of the face-centered-cubic phase of Pd (39).

3.3. Other Metal Membranes. Metal membranes of Ag, Au, Cu, and Ni were also fabricated using the same activation approach. From the SEM-EDX results shown in Figure 4 (30 min plating), it was found that all of the membranes were successfully formed on the activated substrates. From the elemental results, it was found that each coated metal came from the corresponding metal ions in the plating bath. However, the electroless Ni deposits were not pure Ni but contained significant amounts of phosphorus (P). EDX analysis (inset tables) of the deposits showed an average Ni/P mass ratio of 8.4:1. Because the Ni plating bath contained NaH_2PO_2, the resulting deposits were Ni−P par-

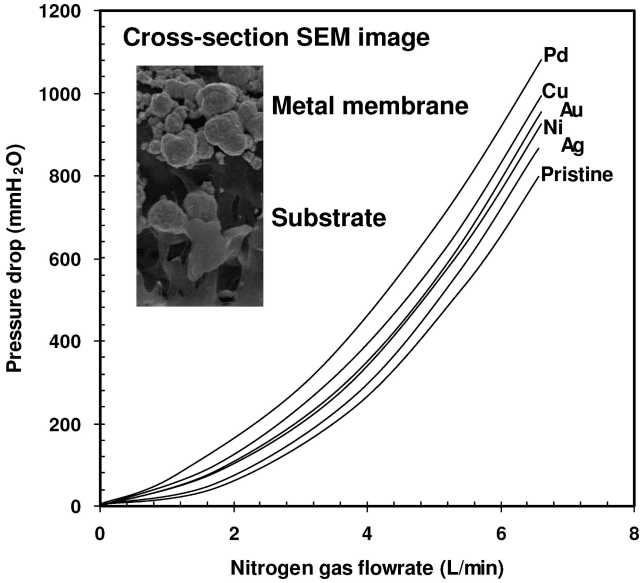

FIGURE 5. Nitrogen gas flow rate vs pressure drop of metal membrane/substrate samples (at 25 °C).

ticles (40, 41). From ICP-AES analyses, the average plating rates of Ag, Au, Cu, and Ni membranes at a plating time of 30 min were 8.2, 33.8, 21.9, and 20.1 $\mu g/cm^2 \cdot$ min, respectively. The dimensional growth rates estimated from AFM analyses were 28, 93, 72, and 64 nm/min for Ag, Au, Cu, and Ni, respectively. The differences in the plating and growth rates were caused by the different compositions and temperatures of plating baths.

The pressure drops across the metal membrane/substrate samples were measured, and as shown in Figure 5, the metal membrane did affect the pressure drop of the pristine substrate. Figure 5 also shows that the increase in the nitrogen gas flow rate, from 1 to 7 L/min, caused an increased pressure drop of the samples from ~50 to ~1000 mmH_2O (from ~30 to 800 mmH_2O for the pristine substrate). Increases of the pressure drop of the samples were caused by the metal membrane; the plated metal membrane could block or take up some channels of the corresponding substrate (inset of Figure 5). On the other hand, the pressure drop did not exactly correlate with the plating rate. This means that the pressure drop may also be affected by morphology or distribution of the metal membrane on a substrate.

4. CONCLUDING REMARKS

Fabrication of a metal membrane on a perforated PTFE substrate was developed by Pd aerosol activation and subsequent Pd ELP. Homogeneous Pd particles on an aerosol-activated substrate with a mean size of 188 nm were packed tightly to form a Pd membrane after Pd plating. When the plating time increased from 10 to 30 min, the thickness increased from 0.4 to 1.6 μm. The average plating rate of Pd was 14.2 $\mu g/cm^2 \cdot$ min for an activation intensity of 25 $\mu g/cm^2$ (Pd/substrate). Other metal membranes (Ag, Au, Cu, and Ni) were fabricated on the activated substrate using different plating baths. When the plating time was 30 min, the average plating rates of the Ag, Au, Cu, and Ni membranes were 8.2, 33.8, 21.9, and 20.1 $\mu g/cm^2 \cdot$ min, respectively.

Acknowledgment. This study was supported by a R&D project from the Korea Energy Management Corp. (KEMCO; Grant 2008-N-PV08-P-06-0-000).

REFERENCES AND NOTES

(1) Kim, J.-W.; Lee, J.-E.; Ryu, J.-H.; Lee, J.-S.; Kim, S.-J.; Han, S.-H.; Chang, I.-S.; Kang, H.-H.; Suh, K.-D. *J. Polym. Sci., Part A* **2004**, *42*, 2551.
(2) Kim, J.-W.; Lee, J.-E.; Kim, S.-J.; Lee, J.-S.; Ryu, J.-H.; Kim, J.; Han, S.-H.; Chang, I.-S.; Suh, K.-D. *Polymer* **2004**, *45*, 4741.
(3) Ishii, D.; Yabu, H.; Shimomura, M. *Colloids Surf. A* **2008**, *313–314*, 590.
(4) Brown, I. J.; Sotiropoulos, S. *J. Appl. Electrochem.* **2001**, *31*, 1203.
(5) Park, K.-W.; Seol, K.-S. *Electrochem. Commun.* **2007**, *9*, 2256.
(6) Adhikari, S.; Fernando, S. *Ind. Eng. Chem. Res.* **2006**, *45*, 875.
(7) Bhuvana, T.; Kumar, G. V. P.; Kulkarni, G. U.; Narayana, C. *J. Phys. Chem. C* **2007**, *111*, 6700.
(8) Yang, L.; Bai, S.; Zhu, D.; Yang, Z.; Zhang, M.; Zhang, Z.; Chen, E.; Cao, W. *J. Phys. Chem. C* **2007**, *111*, 431.
(9) Huang, Y.; Dittmeyer, R. *J. Membr. Sci.* **2007**, *302*, 160.
(10) Touchais-Papet, E.; Charbonnier, M.; Romand, M. *Appl. Surf. Sci.* **1999**, *138–139*, 557.
(11) Yamamoto, Y.; Takeda, S.; Shiigi, H.; Nagaoka, T. *J. Electrochem. Soc.* **2007**, *154*, D462.
(12) Dai, H.; Li, H.; Wang, F. *Surf. Coat. Technol.* **2006**, *201*, 2859.
(13) Wu, L.-Q.; Xu, N.; Shi, J. *Ind. Eng. Chem. Res.* **2000**, *39*, 342.
(14) Chen, D.; Lu, Q.; Zhao, Y. *Appl. Surf. Sci.* **2006**, *253*, 1573.
(15) Pimenov, S. M.; Shafeev, G. A.; Loubnin, E. N. *Appl. Phys. Lett.* **1996**, *68*, 334.
(16) Esrom, H. *Appl. Surf. Sci.* **2000**, *168*, 1.
(17) Kreitz, S.; Penache, C.; Thomas, M.; Klages, C. P. *Surf. Coat. Technol.* **2005**, *200*, 676.
(18) Weller, R. A.; Ryle, W. T.; Newton, A. T.; McMahon, M. D.; Miller, T. M.; Magruder, R. H., III *IEEE Trans. Nanotechnol.* **2003**, *2*, 154.
(19) Gray, J. E.; Norton, P. R.; Griffiths, K. *Thin Solid Films* **2005**, *484*, 196.
(20) Kordás, K.; Békési, J.; Bali, K.; Vajtai, R.; Nánai, L.; George, T. F.; Leppävuori, S. *J. Mater. Res.* **1999**, *14*, 3690.
(21) Weber, A. P.; Seipenbusch, M.; Kasper, G. *J. Phys. Chem. A* **2001**, *105*, 8958.
(22) Byeon, J. H.; Ko, B. J.; Hwang, J. *J. Phys. Chem. C* **2008**, *112*, 3627.
(23) Nunes, S. P.; Peinemann, K.-V. *Membrane Technology in the Chemical Industry*; Wiley-VCH: Weinheim, Germany, 2001.
(24) Chen, J.; Asano, M.; Maekawa, Y.; Yoshida, M. *J. Membr. Sci.* **2006**, *277*, 249.
(25) Liu, Y.-L.; Yu, C.-H.; Lai, J.-Y. *J. Membr. Sci.* **2008**, *315*, 106.
(26) Tu, C.-Y.; Liu, Y.-L.; Lee, K.-R.; Lai, J.-Y. *J. Membr. Sci.* **2006**, *274*, 47.
(27) Tu, C.-Y.; Liu, Y.-L.; Lee, K.-R.; Lai, J.-Y. *Polymer* **2005**, *46*, 6976.
(28) Byeon, J. H.; Park, J. H.; Hwang, J. *J. Aerosol Sci.* **2008**, *39*, 888.
(29) Yin, X.; Hong, L.; Liu, Z.-L. *J. Phys. Chem. C* **2007**, *111*, 9194.
(30) Bryden, K.; Ying, J. *J. Membr. Sci.* **2002**, *203*, 29.
(31) Lo, S. H. Y.; Chen, T.-Y.; Wang, Y.-Y.; Wan, C.-C.; Lee, J.-F.; Lin, T.-L. *J. Phys. Chem. C* **2007**, *111*, 12873.
(32) Jun, C.-S.; Lee, K.-H. *J. Membr. Sci.* **2000**, *176*, 121.
(33) Grashoff, G.; Pilkington, C.; Corti, C. *Platinum Met. Rev.* **1983**, *27*, 157.
(34) Yeung, K. L.; Christiansen, S. C.; Varma, A. *J. Membr. Sci.* **1999**, *159*, 107.
(35) Shi, Z.; Wu, S.; Szpunar, J. A.; Roshd, M. *J. Membr. Sci.* **2006**, *280*, 705.
(36) Persson, K.; Jansson, K.; Järås, S. G. *J. Catal.* **2007**, *245*, 401.
(37) Shi, Z.; Szpunar, J. A. *Rev. Adv. Mater. Sci.* **2007**, *15*, 1.
(38) Schaefers, S.; Rast, L.; Stanishevsky, A. *Mater. Lett.* **2006**, *60*, 706.
(39) French, B. L.; Davis, L. M.; Munzinger, E. S.; Slavin, J. W. J.; Christy, P. C.; Thompson, D. W.; Southward, R. E. *Chem. Mater.* **2005**, *17*, 2091.
(40) Cui, G.; Liu, H.; Wu, G.; Zhao, J.; Song, S.; Shen, P. K. *J. Phys. Chem. C* **2008**, *112*, 4601.
(41) Ishii, D.; Nagashima, T.; Udatsu, M.; Sun, R.-D.; Ishikawa, Y.; Kawasaki, S.; Yamada, M.; Iyoda, T.; Nakagawa, M. *Chem. Mater.* **2006**, *18*, 2152.

AM8001742